

# Growth hormone receptor knockout to reduce the size of donor pigs for preclinical xenotransplantation studies

Arne Hinrichs<sup>1,2</sup>  | Evamaria O. Riedel<sup>3</sup>  | Nikolai Klymiuk<sup>1,2</sup>  |  
 Andreas Blutke<sup>4</sup>  | Elisabeth Kemter<sup>1,2</sup>  | Matthias Längin<sup>5</sup>  | Maik Dahlhoff<sup>1</sup>  |  
 Barbara Keßler<sup>1,2</sup>  | Mayuko Kurome<sup>1,2</sup>  | Valeri Zakhartchenko<sup>1,2</sup>  |  
 Eva-Maria Jemiller<sup>1,2</sup> | David Ayares<sup>6</sup>  | Martin Bidlingmaier<sup>7</sup>  |  
 Florian Flenkenthaler<sup>3</sup>  | Martin Hrabě de Angelis<sup>4</sup>  | Georg J. Arnold<sup>3</sup>  |  
 Bruno Reichart<sup>8</sup>  | Thomas Fröhlich<sup>3</sup>  | Eckhard Wolf<sup>1,2,3</sup> 

<sup>1</sup>Department of Veterinary Sciences, Chair for Molecular Animal Breeding and Biotechnology, Gene Center, LMU Munich, Munich, Germany

<sup>2</sup>Center for Innovative Medical Models (CiMM), LMU Munich, Munich, Germany

<sup>3</sup>Laboratory for Functional Genome Analysis (LAFUGA), Gene Center, LMU Munich, Munich, Germany

<sup>4</sup>Institute of Experimental Genetics, Helmholtz Zentrum München, Chair of Experimental Genetics, Technical University of Munich, Neuherberg, Germany

<sup>5</sup>Department of Anaesthesiology, University Hospital, LMU Munich, Munich, Germany

<sup>6</sup>Revivicor Inc., Blacksburg, VA, USA

<sup>7</sup>Medizinische Klinik und Poliklinik IV, Klinikum der Universität München, Munich, Germany

<sup>8</sup>Walter Brendel Center for Experimental Medicine, LMU Munich, Munich, Germany

## Correspondence

Eckhard Wolf, Gene Center, LMU Munich, Feodor-Lynen-Str. 25, D-81377 Munich, Germany.  
 Email: ewolf@genzentrum.lmu.de

## Present address

Nikolai Klymiuk, Professorship for Large Animals Models in Cardiovascular Research, Technical University of Munich, Munich, Germany

## Abstract

**Background:** Many genetically multi-modified donor lines for xenotransplantation have a background of domestic pigs with rapid body and organ growth. The intrinsic growth potential of porcine xeno-organs may impair their long-term function after orthotopic transplantation in non-human primate models. Since growth hormone is a major stimulator of postnatal growth, we deleted its receptor (*GHR-KO*) to reduce the size of donor pigs in one step.

**Methods:** Heart weight and proteome profile of myocardium were investigated in *GHR-KO* and control pigs. *GHR-KO* mutations were introduced using CRISPR/Cas9 in an  $\alpha 1,3$ -galactosyltransferase (*GGTA1*)-deficient background expressing the human cluster of differentiation (*hCD46*) and human thrombomodulin (*hTHBD*) to generate quadruple-modified (4GM) pigs.

**Results:** At age 6 months, *GHR-KO* pigs had a 61% reduced body weight and a 63% reduced heart weight compared with controls. The mean minimal diameter of cardiomyocytes was 28% reduced. A holistic proteome study of myocardium samples from the two groups did not reveal prominent differences. Two 4GM founder sows had low serum insulin-like growth factor 1 (IGF1) levels ( $24 \pm 1$  ng/mL) and reached body weights of 70.3 and 73.4 kg at 9 months. Control pigs with IGF1 levels of  $228 \pm 24$  ng/mL reached this weight range three months earlier. The 4GM sows showed normal sexual development and were mated with genetically multi-modified boars. Offspring revealed the expected Mendelian transmission of the genetic modifications and consistent expression of the transgenes.

Arne Hinrichs and Evamaria O. Riedel equal first author contribution.

Thomas Fröhlich and Eckhard Wolf equal last author contribution.

This is an open access article under the terms of the Creative Commons Attribution-NonCommercial-NoDerivs License, which permits use and distribution in any medium, provided the original work is properly cited, the use is non-commercial and no modifications or adaptations are made.

© 2020 The Authors. *Xenotransplantation* published by John Wiley & Sons Ltd

Maik Dahlhoff, Institute of in vivo and in vitro models, University of Veterinary Medicine Vienna, Vienna, Austria

#### Funding information

Deutsche Forschungsgemeinschaft, Grant/Award Number: HI 2206/2-1 and TRR 127

**Conclusion:** *GHR*-KO donor pigs can be used at an age beyond the steepest phase of their growth curve, potentially reducing the problem of xeno-organ overgrowth in preclinical studies.

#### KEYWORDS

gene editing, growth hormone receptor, organ growth, pig

## 1 | INTRODUCTION

Xenotransplantation of genetically modified pig hearts reached a milestone on the way to clinical trials by consistent long-term survival of orthotopic xenografts in baboons.<sup>1,2</sup> With hearts from  $\alpha$ 1,3-galactosyltransferase (GGTA1)-deficient pigs expressing the human cluster of differentiation 46 (hCD46) and human thrombomodulin (hTHBD), the recipients survived for up to 195 days. In addition to non-ischemic perfusion preservation of the donor heart and safe immunosuppression of the recipient baboon, post-transplantation growth control of the xenotransplant was essential. This was achieved by lowering the recipient's blood pressure, early weaning of cortisone, and temsirolimus treatment. Discontinuation of mechanistic target of rapamycin (mTOR) inhibition by temsirolimus resulted in immediate growth of the xeno-heart, limiting its function in the small chest of a baboon. The donor animals in these studies had a genetic background of domestic pigs (German Landrace/Large White) and had to be used at juvenile age to fit with the size of the recipient baboons. Continued organ growth has also been observed after allotransplantation of domestic pig kidneys into minipigs<sup>3</sup> or after xenotransplantation into baboons (<sup>3-5</sup>; reviewed in<sup>6</sup>). Pigs (and their organs) grow much faster than non-human primates. To overcome this physiological discrepancy, we sought a way to reduce by gene editing the size of xeno-organ donor pigs in one step.

Inactivation of the growth hormone receptor (*GHR*) gene appeared to be an attractive strategy since *GHR*-deficient mice are small, but fertile and have a prolonged life span.<sup>7,8</sup> Furthermore, *GHR*-deficient patients (Laron syndrome) are also small and have reduced risk to suffer from diabetes or malignancies.<sup>9</sup> We therefore generated *GHR*-deficient (*GHR*-KO) pigs, which exhibit low plasma insulin-like growth factor 1 (IGF1) levels and significantly reduced postnatal body and organ growth, but normal fertility.<sup>10</sup>

The aims of the present study were (a) to quantify effects of *GHR*-KO on cardiac growth parameters including morphometric studies of cardiomyocytes and (b) to screen by holistic label-free proteomics for molecular alterations of myocardium potentially affecting the function of *GHR*-deficient hearts. Furthermore, *GHR*-KO mutations were introduced into a *GGTA1*-KO, *hCD46/hTHBD* double-transgenic genetic background. The phenotype of two female quadruple-modified (4GM) founder pigs was compared with pigs carrying the *GHR*-KO mutation only. After mating with genetically multi-modified boars, the offspring were analyzed for the inheritance of the genetic modifications and for expression of the transgenes.

Our results suggest *GHR*-KO as a feasible strategy to reduce the size of organ donor pigs for preclinical xenotransplantation studies.

## 2 | METHODS

### 2.1 | Animal model and collection of heart muscle samples

All animal procedures were approved by the responsible animal welfare authority (Regierung von Oberbayern; permission ROB-55.2Vet-2532.Vet-02-17-136) and performed according to the German Animal Welfare Act and Directive 2010/63/EU on the protection of animals used for scientific purposes.

Six-month-old *GHR*-KO (4 males and 4 females) and *GHR* expressing control pigs (*GHR*<sup>+/-</sup>, *GHR*<sup>+/+</sup>; 2 males and 2 females per genotype)<sup>10</sup> were euthanized after overnight fasting. Heart muscle samples (left ventricle, right ventricle, ventricular septum) were taken according to a standardized protocol,<sup>11,12</sup> routinely fixed in formalin, and processed for paraffin histology, or shock frozen on dry ice and stored at -80°C.

### 2.2 | Histological measurements

The mean minimal diameters of cardiomyocytes were determined planimetrically (Videoplan-System, Zeiss-Kontron) in systematically randomly sampled fields of view in HE-stained paraffin sections of myocardium samples of the left ventricle (LV), the right ventricle (RV), and the ventricular septum (S). Measurements were performed in a blinded fashion, that is, the examiner was not aware of the genotype-affiliations of the examined sections. Per case, 318 ± 61 fiber profiles were analyzed.

### 2.3 | Proteomics

Pressure-assisted lysis and digestion of proteins were performed using a Barocycler 2320 EXT (Pressure BioSciences). For tissue lysis, 2 mg frozen muscle tissue, 20  $\mu$ L 6 mol/L urea/100 mmol/L  $\text{NH}_4\text{HCO}_3$  and 1:50 (enzyme:substrate) lysyl endopeptidase (Fujifilm Wako) were added to the microtubes closed with a micro-pestle. Subsequently, 90 cycles of 45 kpsi at 35°C were applied. Proteins were reduced at a final concentration of 4.5 mmol/L dithioerythritol

(DTE)/2 mmol/L tris(2-carboxyethyl)phosphine (TCEP) for 30 minutes at 56°C. Cysteine residues were blocked for 30 minutes in the dark at a final concentration of 8.3 mmol/L iodoacetamide. Samples were diluted to a concentration of 0.8 mol/L urea with 50 mmol/L  $\text{NH}_4\text{HCO}_3$ /10% n-propanol. For protein digestion, 1:50 (enzyme:substrate) porcine trypsin (Promega) was added to the microtubes closed with the microcaps. Subsequently, 90 cycles of 20 kpsi at 35°C were applied.

The LC-MS/MS system comprised an UltiMate™ 3000 RSLCnano chromatography system (Thermo Scientific) connected to a Q Exactive HF-X mass spectrometer (Thermo Scientific). One  $\mu\text{g}$  of peptides diluted in 0.1% formic acid (FA) was transferred to a 2-cm trap column (Acclaim® PepMap 100, 75  $\mu\text{m}$   $\times$  2 cm, nanoViper C18, 3  $\mu\text{m}$ , 100 Å, Thermo Scientific) and separated using consecutive linear gradients at a flow rate of 250 nL/min on a 50-cm separation column (PepMap® RSLC, 75  $\mu\text{m}$   $\times$  50 cm, nanoViper C18, 2  $\mu\text{m}$ , 100 Å, Thermo Scientific). The LC gradients were from 3% to 25% solvent B (0.1% FA, 100% acetonitrile (ACN)) in 160 minutes followed by 25% to 40% solvent B in 10 minutes, and 40% to 85% solvent B in 10 minutes. MS acquisition cycles comprised one full MS scan at a resolution of 60 000 and 15 data-dependent higher collision dissociation (HCD) MS/MS scans at a resolution of 15 000 and a collision energy of 28. The dataset was submitted to the ProteomeXchange Consortium via the PRIDE partner repository<sup>13</sup> with the identifier PXD019852.

For label-free quantification (LFQ),<sup>14</sup> data were processed using MaxQuant V1.6.2.10, Perseus V1.6.1.3, and the Sus scrofa subset of the NCBI database (NCBI RefSeq Sus scrofa Annotation Release 106 Sscrofa 11.1). As parameters for identification (false discovery rate < 0.01), we used trypsin as enzyme, a mass tolerance of the precursor of 10 ppm, a MS/MS mass tolerance of 0.02 Da, carbamidomethylation of cysteine as fixed modification and oxidized methionine as variable modifications. In cases where proteins were detected in all replicates of one group, but in no replicate of the other group, the MaxQuant imputation feature was applied to allow statistical evaluation. Hierarchical clustering, 2D principal component analysis, and volcano plot analysis were carried out using the algorithms implemented in Perseus.<sup>15</sup>

## 2.4 | Generation of *GHR*-KO, *GGTA1*-KO, and *hCD46/hTHBD* double-transgenic (4GM) pigs

Primary kidney cells were isolated from a female *GGTA1*<sup>-/-</sup>, *hCD46/hTHBD* double-transgenic pig (both transgenes hemizygous). This triple-modified background is based on a transgene locus with multiple copies of an *hCD46* minigene,<sup>16</sup> which was crossed on a *GGTA1*<sup>-/-</sup> genetic background<sup>17</sup>; later an expression cassette for *hTHBD* under the transcriptional control of a porcine *THBD* regulatory sequence was added.<sup>18</sup> The multicopy *hCD46* cluster was localized by fluorescence *in situ* hybridization (FISH) analysis (Cell Line Genetics) on chromosome 18q11, which

was confirmed by targeted locus amplification (TLA) technology (Cergentis). The transgene integration site of *hTHBD* was revealed by nanopore sequencing (Oxford Nanopore Technologies) on chromosome 9, 73.189 Mb (Sscrofa 11.1. reference genome), in the intronic region between exons 20 and 21 of the *VPS50* gene. Triple-modified cells were co-transfected using a Cas9 expression plasmid (CMV-Cas9<sup>19</sup>) and a plasmid transcribing the *tcatgcactg-gacaGAtgGGG* gRNA (PAM underlined), specific for the porcine *GHR* exon 3. Single-cell clones were produced; PCR products from the porcine *GHR* gene were amplified with the primer pair 5'-gcacacttcagatgctactctaa and 5'-cacatgctcacctcagatac; Sanger sequencing of the PCR product was performed and analyzed for frameshift mutations by bi-directional Sanger sequencing, using the primers 5'-accgctctgaagctgtgacc and 5'-caggagaccagagacctatct. A cell clone carrying a bi-allelic constellation of deleterious mutations was used for somatic cell nuclear transfer (SCNT).<sup>20</sup>

Recipient gilts were synchronized in the estrous cycle by oral administration of 20 mg Altrenogest (Regumate®; MSD Animal Health) per day for 15 days, followed by intramuscular injection of 150  $\mu\text{g}$  Peforelin (Maprelin®; Provet AG) and 750 IU HCG (Ovogest®; MSD Animal Health) after additional 24 and 104 hours, respectively. Embryo transfer was performed laparoscopically into one oviduct.<sup>20</sup> Pregnancy was confirmed by ultrasonographic examination first on day 21 and again 4-6 weeks later.

Genomic DNA was isolated from tail tips of piglets using the Wizard DNA Extraction Kit (Promega). *GHR* mutations were detected by sequencing a *GHR* exon 3 PCR product obtained using primers *GHR*\_Fw 5'-acc gct ctg aag ctg tga cc-3' and *GHR*\_Rv 5'-cac cct cag ata ctc tca tgc-3'. Based on the detected mutations, an *XcmI* restriction fragment length polymorphism assay was established, yielding fragments of 203 bp and 441 bp for wild-type *GHR* and a single fragment of 644 bp for the mutated *GHR* sequence.

## 2.5 | Immunohistochemistry

Tissue samples were fixed in 4% formalin overnight and paraffin-embedded; 3- $\mu\text{m}$  sections were cut and dried. Heat-induced antigen retrieval was performed in Target Retrieval solution (S1699, DAKO) in a boiling water bath for 20 minutes (*hCD46*,  $\alpha\text{Gal}$ ) or in citrate buffer, pH 6.0, in a steamer for 45 minutes (*hTHBD*). Immunohistochemistry was performed using the following primary antibodies: mouse anti-human CD46 monoclonal antibody (HM2103, Hycult Biotech), mouse anti-human thrombomodulin monoclonal antibody (sc-13164, Santa Cruz), and mouse anti- $\alpha\text{Gal}$  IgM (Alx 801-090, Alexis). As secondary antibodies, biotinylated AffiniPure goat anti-mouse IgG (115-065-146, Jackson ImmunoResearch) or biotinylated goat anti-mouse IgM (BA-2020, Vector) were used. Immunoreactivity was visualized using the Vectastain® Elite ABC-HRP Kit (Vector) and 3,3'-diaminobenzidine tetrahydrochloride dihydrate (DAB) as chromogen (brown color). Nuclear counterstaining was done with hemalum (blue color).

## 2.6 | Quantification of serum IGF1 levels

IGF1 concentrations were measured using the iSYS automated chemiluminescent IGF1 assay (Immunodiagnostic Systems) as described previously.<sup>21,22</sup>

## 2.7 | Statistical analysis

Statistical analyses were performed using R<sup>23</sup> with the qvalue package and SAS (SAS Institute) as well as GraphPad Prism (GraphPad Software). Visualizations were performed using R with the ggplot2<sup>24</sup> and pheatmap packages and GraphPad Prism. Effects of group (*GHR*-KO, control), sex, and the interaction group  $\times$  sex were evaluated using two-way ANOVA.

## 3 | RESULTS

### 3.1 | Body weight, heart weight, and cardiomyocyte diameter

At age 6 months, *GHR*-KO pigs had a 61% reduced body weight (Figure 1A;  $P < .0001$ ) and a 63% reduced heart weight compared with controls (Figure 1B;  $P < .0001$ ). The relative heart weight was not different between the two groups (Figure 1C). The mean minimal diameter of cardiomyocytes was 28% reduced in *GHR*-KO vs control

pigs (Figure 1D;  $P < .001$ ). Representative histological sections of myocardium are shown in Figure 1E. None of these parameters was significantly influenced by the animal sex.

### 3.2 | Proteome findings in myocardium

In total, 1,642 protein groups at a false discovery rate (FDR)  $< 0.01$  could be identified. All detected proteins are listed in Table S1A. As a quality control and to check the reproducibility of the approach, multi-scatterplots of MaxQuant intensity values were generated. Mean Pearson correlation coefficients of  $>0.94$  within group were obtained, demonstrating the reproducibility of the results (Figure S1). *GHR*<sup>+/-</sup> and *GHR*<sup>+/+</sup> animals were pooled as control group, since neither phenotypical analysis<sup>10</sup> nor proteome profiling of the liver<sup>25</sup> did show significant differences between these genotypes.

When comparing the quantitative proteome profiles of myocardium samples from *GHR*-KO (4 males and 4 females) and control pigs (4 males and 4 females), neither principal component analysis (Figure 2A) nor hierarchical clustering did result in defined clusters (Figure 2B) indicating no major aberration in the myocardium proteome as a consequence of *GHR* deficiency. Furthermore, statistical analysis of the proteome data using a two-way ANOVA (group  $\times$  sex) identified no protein groups that were significantly ( $P < 0.05$ ) altered in abundance by group, sex or by the interaction group  $\times$  sex (Table S1B). However, a less stringent volcano plot analysis of *GHR*-KO vs WT proteomes, where data were analyzed

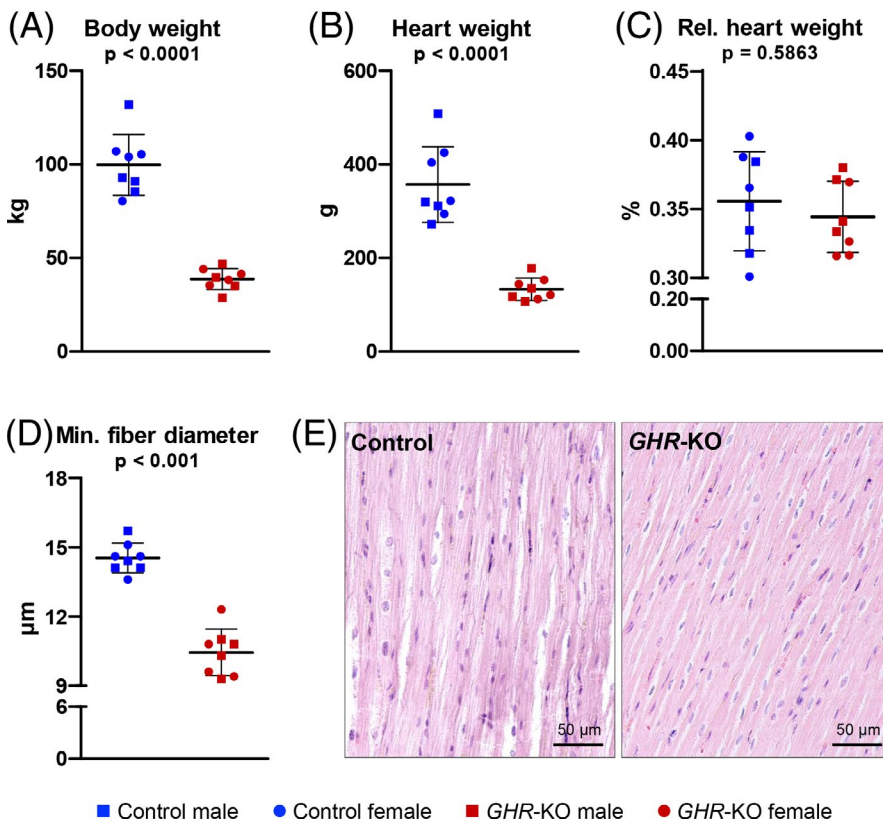
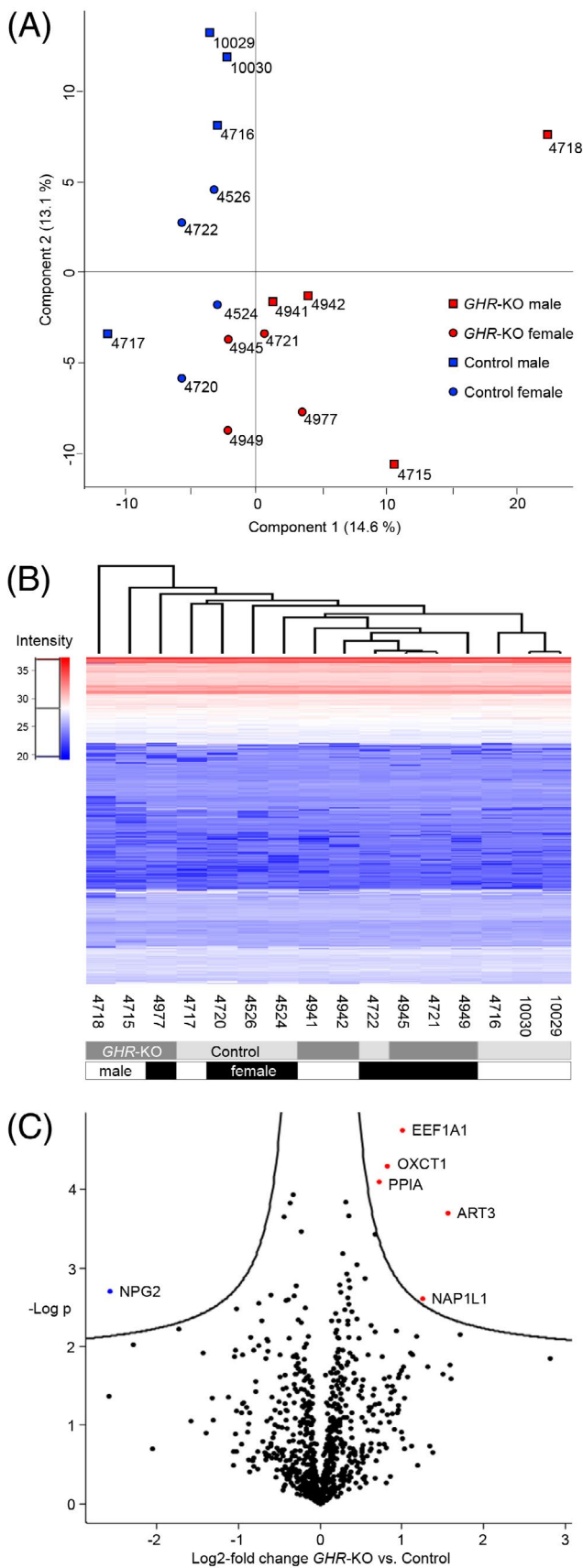


**FIGURE 1** Body weights and heart weights of 6-month-old *GHR*-KO pigs (4 males and 4 females) and controls (4 males and 4 females). A, Body weight; B, Heart weight; C, Relative heart weight; D, Mean minimal diameter of cardiomyocytes; E, Representative histological sections of myocardium.  $P$ -values are from two-way ANOVA for the effect of group (*GHR*-KO, control). Sex and the interaction group  $\times$  sex had no significant effect



without considering the gender, revealed 5 proteins with increased and one protein with reduced abundance in *GHR-KO* vs control myocardium (Figure 2C).

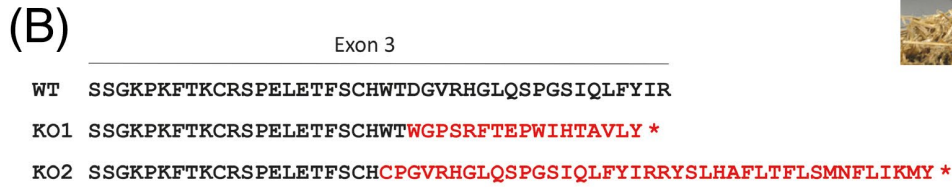
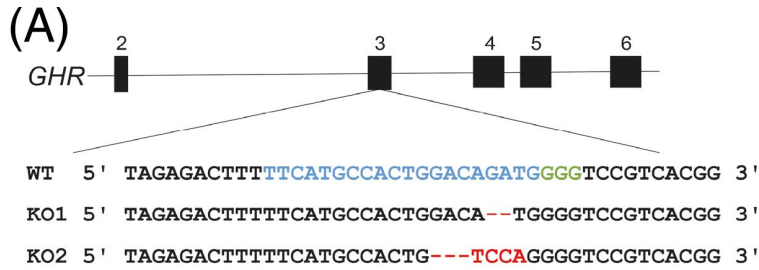
**FIGURE 2** Proteomics of myocardium samples from 6-month-old *GHR-KO* pigs and controls. A, Principal component analysis (PCA); B, Heat map; C, Volcano plot. Proteins with significant abundance changes ( $FDR < 0.05$ ) are labeled: ART3 = ecto-ADP-ribosyltransferase 3; EEF1A1 = elongation factor 1-alpha; NAP1L1 = nucleosome assembly protein 1-like 1; NPG2 = protegrin-2; OXCT13 = oxoacid CoA-transferase 1; PPIA = peptidylprolyl isomerase A. The 4- and 5-digit numbers are individual animal numbers.

### 3.3 | *GHR-KO* pigs with a *GGTA1-KO*, *hCD46/hTHBD* double-transgenic background

A *GGTA1-KO*, *hCD46/hTHBD* double-transgenic cell clone with frameshift mutations in both alleles of the *GHR* gene (Figure 3A) was selected for SCNT. The frameshift mutations result in premature stop codons (Figure 3B) and the complete absence of *GHR*. After transfer of SCNT embryos to recipients, four piglets were born. Two of them died on the first postnatal day; the other two pigs were raised to adulthood without clinical problems (Figure 3C). These exhibited the characteristic phenotype of *GHR* deficiency and reduced serum IGF1 levels ( $24 \pm 1$  ng/mL; mean  $\pm$  SEM), comparable to *GHR-KO* 1GM pigs ( $23 \pm 5$  ng/mL). Serum IGF1 levels of contemporary wild-type pigs were  $215 \pm 58$  ng/mL (Figure 3D). At 9 months, the body weights of the 4GM pigs were 70.3 and 73.4 kg, while wild-type pigs reached this weight range three months earlier. The two 4GM sows showed normal sexual development and were mated with genetically multi-modified boars. The resulting offspring showed the expected Mendelian segregation of the genetic modifications (Figure 3E). Immunohistochemical analysis of myocardium from a *GHR*<sup>+/-</sup>, *GGTA1*<sup>-/-</sup>, *hCD46/hTHBD* double-transgenic pig (Figure 3F) and of ear skin samples from the 4GM founder pigs (Figure S2) revealed the absence of  $\alpha$ Gal epitopes and consistent expression of *hCD46* and *hTHBD*.

## 4 | DISCUSSION

For a number of reasons, including anatomical and physiological similarities with humans, the possibility of efficient and precise genetic engineering, and maintenance under designated pathogen-free conditions, pigs have become the most likely donors of cells, tissues, and organs for xenotransplantation (reviewed in<sup>26</sup>). Many genetically multi-modified pig lines have been established on the background of domestic pigs, which have been selected for decades to maximize growth rate and feed efficiency. As a consequence, the growth rates of porcine organs do not fit with the requirements of non-human primates used as recipients in preclinical xenotransplantation experiments. Even for humans, organs from domestic pigs may grow too large. One possibility to overcome this problem is the use of minipig lines, which may have other drawbacks, for example, high copy numbers of porcine endogenous retroviruses (PERV)<sup>27</sup> or insufficient organ sizes for adult human recipients. Another possibility is genetic engineering of domestic pigs to reduce their growth rate.



(C)

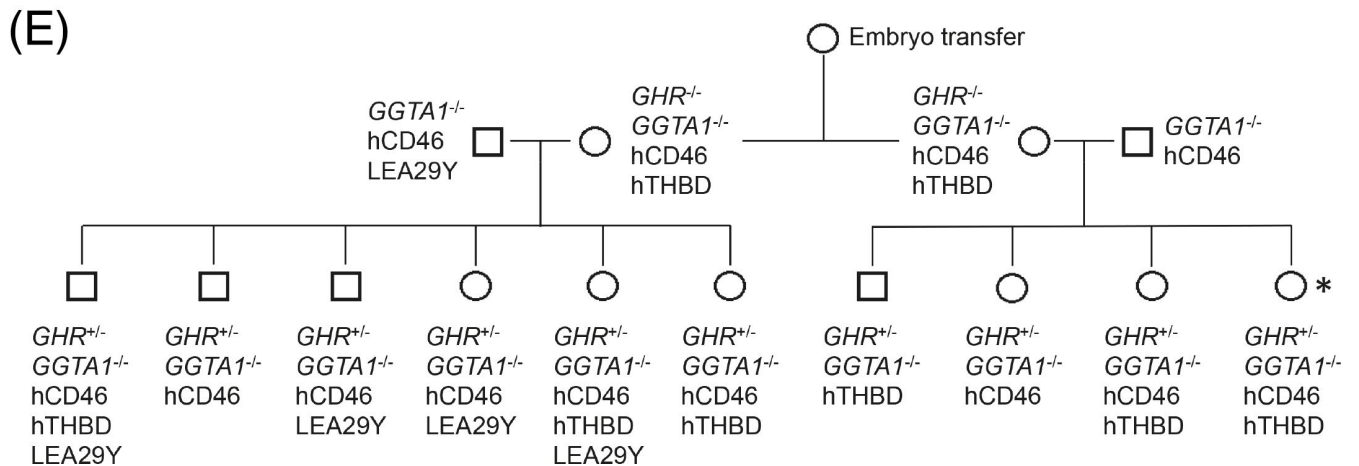
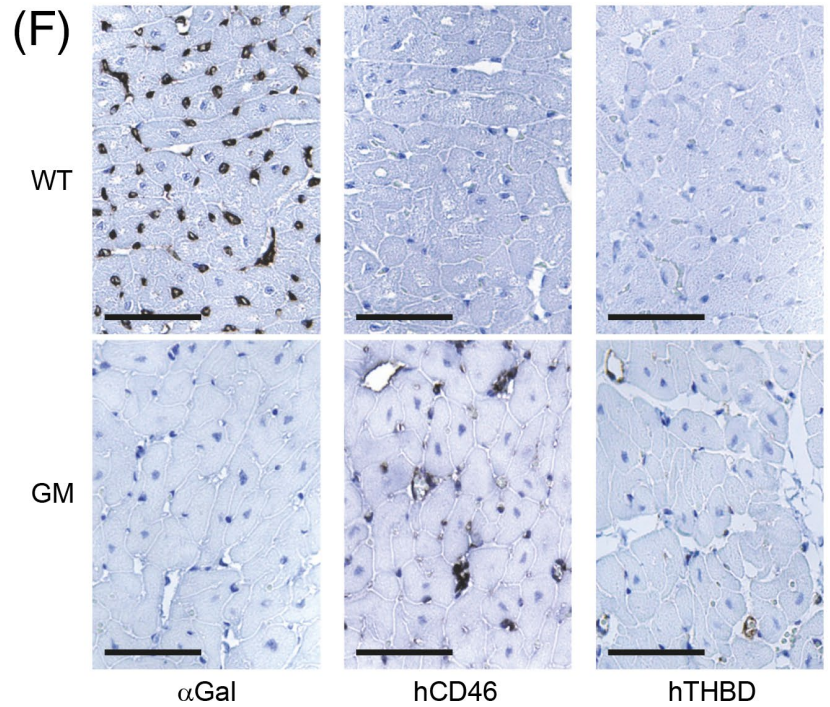
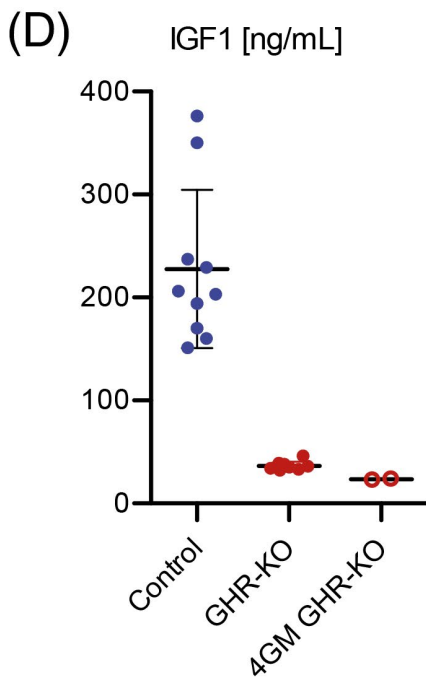


**FIGURE 3** *GHR*-KO pigs with a *GGTA1*-KO, *hCD46/hTHBD* double-transgenic background (4GM). A, Frameshift mutations introduced in exon 3 of the *GHR* gene. B, Premature stop codons (\*) resulting from the frameshift mutations. C, Female 4GM founder pigs. D, Serum IGF1 concentrations. E, Pedigrees resulting from mating of the 4GM founder sows with genetically multi-modified boars. Transgenic animals with *hTHBD*<sup>18</sup> and *LEA29Y*<sup>47</sup> are hemizygous, those with *hCD46* are hemizygous (founder generation) or either hemi- or homozygous (offspring). F, Immunohistochemical staining of  $\alpha$ Gal, *hCD46* and *hTHBD* in myocardium samples from a *GHR*<sup>+/-</sup>, *GGTA1*-KO, *hCD46/hTHBD* double-transgenic pig (GM; labeled with an asterisk in panel E) and a wild-type control (WT). Bars = 50  $\mu$ m

Growth hormone is the major stimulator of postnatal body and organ growth. Excess GH with juvenile or adult onset causes gigantism or acromegaly, respectively (reviewed in<sup>28</sup>), whereas deficiency of GH or its receptor results in reduced body and organ growth (reviewed in<sup>29</sup>). To reduce the size of organ donor pigs, we decided to inactivate the *GHR* gene since the consequences of this condition have been extensively studied in systemic and tissue-specific *Ghr* knockout mice (reviewed in<sup>30,31</sup>) and in *GHR*-deficient patients (Laron syndrome) (reviewed in<sup>29,32</sup>).

To characterize the consequences of *GHR* deficiency in pigs, we introduced frameshift mutations in exon 3 of the porcine *GHR* gene using CRISPR/Cas9.<sup>10</sup> *GHR*-KO pigs resemble the phenotype of human Laron syndrome, including low IGF1 levels, reduced postnatal body and organ growth, an increased proportion of body fat, but no pathological alterations of the blood lipid levels. Moreover, *GHR*-KO pigs are fertile.<sup>10</sup> Significantly reduced body and heart weights of *GHR*-KO pigs were confirmed in a different set of animals in the present study. In addition, the mean minimal diameter of cardiomyocytes was determined, revealing significantly reduced values for *GHR*-KO pigs, which explain—at least in part—their smaller heart size and weight.

A holistic proteome analysis of myocardium samples was performed to screen for prominent molecular changes potentially caused by *GHR* deficiency. In contrast to liver samples from the same set of animals, where multiple proteome differences between *GHR*-KO and control pigs were revealed,<sup>25</sup> the myocardial proteome profiles did not clearly cluster according to group or sex. Furthermore, two-way ANOVA did not identify proteins whose abundance was significantly affected by group, sex, or the interaction group  $\times$  sex. However, a less stringent *t* test based volcano plot analysis revealed 6 proteins with significant abundance differences between myocardium samples from *GHR*-KO vs control pigs.

Increased in abundance were the enzymes ecto-ADP-ribosyltransferase 3 (ART3, reviewed in<sup>33</sup>), 3-oxoacid CoA-transferase 1 (OXCT1, reviewed in<sup>34</sup>) and peptidylprolyl isomerase A (PPIA, reviewed in<sup>35</sup>) as well as elongation factor 1-alpha (EEF1A1, reviewed in<sup>36</sup>) and nucleosome assembly protein 1-like 1 (NAP1L1, reviewed in<sup>37</sup>). Exclusively protegrin-2 (NPG2), a leukocyte-derived peptide with antimicrobial activity,<sup>38</sup> was found to be significantly decreased in *GHR*-KO myocardium. However, none of these proteins is specifically expressed in the myocardium or directly involved in heart contraction. Moreover, none of these proteins is known to be directly regulated by or involved in GH/IGF1 pathways in the heart.

In contrast to the subtle proteome changes in myocardium, there were prominent differences between liver samples of *GHR*-KO and control pigs (same set of animals).<sup>25</sup> Specifically, *GHR* deficiency

resulted in an increased abundance of enzymes involved in amino acid degradation, in the urea cycle, and in the tricarboxylic acid cycle. Additional analyses of acylcarnitine profiles provided evidence for reduced mitochondrial import of fatty acids for beta-oxidation. Moreover, the abundances of several proteins functionally linked to non-alcoholic fatty liver disease (fetuin B, retinol-binding protein 4, and several mitochondrial proteins) were increased. In addition, distinct changes in the methionine and glutathione metabolic pathways were noted. These findings underline the central role of GH to regulate multiple metabolic pathways in the liver (reviewed in<sup>39,40</sup>).

IGF1 is involved in multiple processes in the heart, including contractility, metabolism, hypertrophy, autophagy, senescence, and apoptosis. Moreover, low IGF1 levels are associated with an increased risk of cardiovascular disease (reviewed in<sup>41</sup>). A holistic proteome study of myocardium from *GHR*-deficient individuals with low IGF1 levels has to our knowledge not been performed. Our proteomics data did not provide evidence for substantial molecular changes in the myocardium of *GHR*-KO pigs, which would indicate developmental disturbances or functional abnormalities of the heart. However, the animals were only 6 months old, and it will be important to monitor cardiac function of older *GHR*-KO pigs in the future. Notably, a cardiac-specific inducible knockout of *Ghr* in 4-month-old mice did not affect heart function, as revealed by baseline and post-dobutamine stress test echocardiography and by longitudinal blood pressure measurements.<sup>42</sup> Patients with Laron syndrome were shown to have reduced cardiac dimensions and output but normal left ventricular (LV) ejection fraction at rest and LV contractile reserve following stress.<sup>43</sup>

In our previous orthotopic xenotransplantation studies in baboons, we used donor pigs in the body weight range of 10–34 kg.<sup>44</sup> *GHR*-intact landrace hybrid pigs are in this weight range for less than 2 months (age 41–95 days), whereas *GHR*-KO pigs stay within this weight range for more than 3 months (age 81–181 days)<sup>10</sup> (Figure S3).

To generate small organ donor pigs, we introduced by CRISPR/Cas9 frameshift mutations in female *GGTA1*-KO, *hCD46/hTHBD* double-transgenic cells and used them for SCNT. The two resulting founder pigs with four genetic modifications (4GM) were phenotypically similar to *GHR*-KO 1GM pigs, for example, in postnatal growth rate and serum IGF1 levels. Both sows became sexually mature and were mated with genetically multi-modified boars. Genotyping of the offspring demonstrated the expected Mendelian segregation of the genetic modifications. One of the offspring was subjected to necropsy to evaluate the absence of  $\alpha$ Gal epitopes and the expression of *hCD46* and *hTHBD* in heart and skin samples. The expression patterns of both transgenes were consistent with those reported for *GGTA1*-KO, *hCD46/hTHBD* double-transgenic pigs without *GHR*-KO.<sup>1</sup>

An open question is what will happen to a GHR-deficient organ if it is xenotransplanted into a host with normal IGF1 levels. Observations in liver-specific *Igf1* knockout mice suggest that local IGF1 levels (that would be low in a GHR-KO organ) are more important for organ growth than circulating IGF1, which is mainly derived from the liver.<sup>45</sup>

## 5 | CONCLUSION

In summary, GHR-KO appears to be a feasible approach to reduce the size of xeno-organ donor pig lines in one step without apparent deleterious effects on health and fertility. In addition to preclinical xenotransplantation experiments into non-human primates, this strategy may also be important to provide xeno-hearts for pediatric patients suffering from early onset dilated cardiomyopathy or severe congenital cardiac malformations (reviewed in<sup>46</sup>). A clear advantage of GHR-KO pigs is that the donors can be used at an older age when they have already passed the steepest phase of their growth curve.

## ACKNOWLEDGMENTS

This study was supported by the Deutsche Forschungsgemeinschaft (TRR127, HI 2206/2-1). Oxford nanopore sequencing was performed by Stefan Krebs, Andreas Hauser, and Helmut Blum, Laboratory for Functional Genome Analysis (LAFUGA), Gene Center, LMU Munich. The authors gratefully acknowledge excellent technical support by Christina Blechinger, Christian Eckardt, Christian Erdle, Tuna Güngör, Sylvia Hering, Harald Paul, and Tatjana Schröter. Open access funding enabled and organized by Projekt DEAL.

## CONFLICT OF INTEREST

David Ayares is chief executive officer and chief scientific officer of Revivacor Inc. The other authors have no conflicts of interest to disclose.

## ORCID

Arne Hinrichs  <https://orcid.org/0000-0003-3022-5983>  
 Evamaria O. Riedel  <https://orcid.org/0000-0003-2259-9221>  
 Nikolai Klymiuk  <https://orcid.org/0000-0003-3532-1659>  
 Andreas Blutke  <https://orcid.org/0000-0001-7824-2681>  
 Elisabeth Kemter  <https://orcid.org/0000-0001-7785-7502>  
 Matthias Längin  <https://orcid.org/0000-0003-0996-4941>  
 Maik Dahlhoff  <https://orcid.org/0000-0001-9189-7631>  
 Barbara Keßler  <https://orcid.org/0000-0001-7036-238X>  
 Mayuko Kurome  <https://orcid.org/0000-0002-2725-8613>  
 Valeri Zakhartchenko  <https://orcid.org/0000-0002-5974-9759>  
 David Ayares  <https://orcid.org/0000-0002-4638-3321>  
 Martin Bidlingmaier  <https://orcid.org/0000-0002-4681-6668>  
 Florian Flenkenthaler  <https://orcid.org/0000-0003-2964-9236>  
 Martin Hrabě de Angelis  <https://orcid.org/0000-0002-7898-2353>  
 Georg J. Arnold  <https://orcid.org/0000-0002-2716-0229>  
 Bruno Reichart  <https://orcid.org/0000-0003-2859-3664>  
 Thomas Fröhlich  <https://orcid.org/0000-0002-4709-3211>  
 Eckhard Wolf  <https://orcid.org/0000-0002-0430-9510>

## REFERENCES

- Längin M, Mayr T, Reichart B, et al. Consistent success in life-supporting porcine cardiac xenotransplantation. *Nature*. 2018;564(7736):430-433.
- Reichart B, Längin M, Radan J, et al. Pig-to-non-human primate heart transplantation: The final step toward clinical xenotransplantation? *J Heart Lung Transplant*. 2020;39(8):751-757.
- Tanabe T, Watanabe H, Shah JA, et al. Role of intrinsic (graft) versus extrinsic (host) factors in the growth of transplanted organs following allogeneic and xenogeneic transplantation. *Am J Transplant*. 2017;17(7):1778-1790.
- Iwase H, Liu H, Wijkstrom M, et al. Pig kidney graft survival in a baboon for 136 days: longest life-supporting organ graft survival to date. *Xenotransplantation*. 2015;22(4):302-309.
- Iwase H, Hara H, Ezzelarab M, et al. Immunological and physiological observations in baboons with life-supporting genetically engineered pig kidney grafts. *Xenotransplantation*. 2017;24(2):e12293.
- Iwase H, Cooper DK. Growth hormone receptor knockout: relevance to xenotransplantation. *Xenotransplantation*. 2020; e12652 (accepted).
- Zhou Y, Xu BC, Maheshwari HG, et al. A mammalian model for Laron syndrome produced by targeted disruption of the mouse growth hormone receptor/binding protein gene (the Laron mouse). *Proc Natl Acad Sci U S A*. 1997;94(24):13215-13220.
- Coschigano KT, Clemmons D, Bellush LL, Kopchick JJ. Assessment of growth parameters and life span of GHR/BP gene-disrupted mice. *Endocrinology*. 2000;141(7):2608-2613.
- Guevara-Aguirre J, Balasubramanian P, Guevara-Aguirre M, et al. Growth hormone receptor deficiency is associated with a major reduction in pro-aging signaling, cancer, and diabetes in humans. *Sci Transl Med*. 2011;3(70):70ra13.
- Hinrichs A, Kessler B, Kurome M, et al. Growth hormone receptor-deficient pigs resemble the pathophysiology of human Laron syndrome and reveal altered activation of signaling cascades in the liver. *Mol Metab*. 2018;11:113-128.
- Albl B, Haesner S, Braun-Reichhart C, et al. Tissue sampling guides for porcine biomedical models. *Toxicol Pathol*. 2016;44(3):414-420.
- Blutke A, Renner S, Flenkenthaler F, et al. The munich MIDY pig biobank - a unique resource for studying organ crosstalk in diabetes. *Mol Metab*. 2017;6(8):931-940.
- Perez-Riverol Y, Csordas A, Bai J, et al. The PRIDE database and related tools and resources in 2019: improving support for quantification data. *Nucleic Acids Res*. 2019;47(D1):D442-d450.
- Cox J, Hein MY, Luber CA, Paron I, Nagaraj N, Mann M. Accurate proteome-wide label-free quantification by delayed normalization and maximal peptide ratio extraction, termed MaxLFQ. *Mol Cell Proteomics*. 2014;13(9):2513-2526.
- Tyanova S, Temu T, Sinitcyn P, et al. The Perseus computational platform for comprehensive analysis of (prote)omics data. *Nat Methods*. 2016;13(9):731-740.
- Loveland BE, Milland J, Kyriakou P, et al. Characterization of a CD46 transgenic pig and protection of transgenic kidneys against hyperacute rejection in non-immunosuppressed baboons. *Xenotransplantation*. 2004;11(2):171-183.
- Phelps CJ, Koike C, Vaught TD, et al. Production of alpha 1,3-galactosyltransferase-deficient pigs. *Science*. 2003;299(5605):411-414.
- Wuensch A, Baehr A, Bongoni AK, et al. Regulatory sequences of the porcine THBD gene facilitate endothelial-specific expression of bioactive human thrombomodulin in single- and multitransgenic pigs. *Transplantation*. 2014;97(2):138-147.
- Mali P, Yang L, Esvelt KM, et al. RNA-guided human genome engineering via Cas9. *Science*. 2013;339(6121):823-826.
- Kurome M, Kessler B, Wuensch A, Nagashima H, Wolf E. Nuclear transfer and transgenesis in the pig. *Methods Mol Biol*. 2015;1222:37-59.



21. Bidlingmaier M, Friedrich N, Emeny RT, et al. Reference intervals for insulin-like growth factor-1 (igf-i) from birth to senescence: results from a multicenter study using a new automated chemiluminescence IGF-I immunoassay conforming to recent international recommendations. *J Clin Endocrinol Metab.* 2014;99(5):1712-1721.
22. Hofmann I, Kemter E, Theobalt N, et al. Linkage between growth retardation and pituitary cell morphology in a dystrophin-deficient pig model of Duchenne muscular dystrophy. *Growth Horm IGF Res.* 2020;51:6-16.
23. Team RC. *R: A language and environment for statistical computing.* Vienna, Austria: R foundation for statistical computing. 2013.
24. Wickham H. *ggplot2: elegant graphics for data analysis.* New York: Springer; 2016.
25. Riedel EO, Hinrichs A, Kemter E, et al. Functional changes of the liver in the absence of growth hormone (GH) action - Proteomic and metabolomic insights from a GH receptor deficient pig model. *Mol Metab.* 2020;36:100978.
26. Kemter E, Schnieke A, Fischer K, Cowan PJ, Wolf E. Xeno-organ donor pigs with multiple genetic modifications - the more the better? *Curr Opin Genet Dev.* 2020;64:60-65.
27. Semaan M, Rotem A, Barkai U, Bornstein S, Denner J. Screening pigs for xenotransplantation: prevalence and expression of porcine endogenous retroviruses in Göttingen minipigs. *Xenotransplantation.* 2013;20(3):148-156.
28. Beckers A, Petrossians P, Hanson J, Daly AF. The causes and consequences of pituitary gigantism. *Nat Rev Endocrinol.* 2018;14(12):705-720.
29. Aguiar-Oliveira MH, Bartke A. Growth hormone deficiency: health and longevity. *Endocr Rev.* 2019;40(2):575-601.
30. List EO, Duran-Ortiz S, Kopchick JJ. Effects of tissue-specific GH receptor knockouts in mice. *Mol Cell Endocrinol.* 2020;515:110919.
31. Basu R, Qian Y, Kopchick JJ. Mechanisms in Endocrinology: lessons from growth hormone receptor gene-disrupted mice: are there benefits of endocrine defects? *Eur J Endocrinol.* 2018;178(5):R155-r181.
32. Laron Z. Lessons from 50 years of study of Laron syndrome. *Endocr Pract.* 2015;21(12):1395-1402.
33. Grahner A, Grahner A, Klein C, Schilling E, Wehrhahn J, Hauschildt S. Review: NAD<sup>+</sup>: a modulator of immune functions. *Innate Immun.* 2011;17(2):212-233.
34. Fukao T, Mitchell G, Sass JO, Hori T, Orii K, Aoyama Y. Ketone body metabolism and its defects. *J Inherit Metab Dis.* 2014;37(4):541-551.
35. Rostam MA, Piva TJ, Rezaei HB, et al. Peptidyl-prolyl isomerases: functionality and potential therapeutic targets in cardiovascular disease. *Clin Exp Pharmacol Physiol.* 2015;42(2):117-124.
36. Sasikumar AN, Perez WB, Kinzy TG. The many roles of the eukaryotic elongation factor 1 complex. *Wiley Interdiscip Rev RNA.* 2012;3(4):543-555.
37. Attia M, Rachez C, Avner P, Rogner UC. Nucleosome assembly proteins and their interacting proteins in neuronal differentiation. *Arch Biochem Biophys.* 2013;534(1-2):20-26.
38. Harwig SS, Swiderek KM, Lee TD, Lehrer RI. Determination of disulphide bridges in PG-2, an antimicrobial peptide from porcine leukocytes. *J Pept Sci.* 1995;1(3):207-215.
39. Vijayakumar A, Yakar S, Leroith D. The intricate role of growth hormone in metabolism. *Front Endocrinol (Lausanne).* 2011;2:32.
40. Vijayakumar A, Novosyadlyy R, Wu Y, Yakar S, LeRoith D. Biological effects of growth hormone on carbohydrate and lipid metabolism. *Growth Horm IGF Res.* 2010;20(1):1-7.
41. Troncoso R, Ibarra C, Vicencio JM, Jaimovich E, Lavandero S. New insights into IGF-1 signaling in the heart. *Trends Endocrinol Metab.* 2014;25(3):128-137.
42. Jara A, Liu X, Sim D, et al. Cardiac-specific disruption of GH receptor alters glucose homeostasis while maintaining normal cardiac performance in adult male mice. *Endocrinology.* 2016;157(5):1929-1941.
43. Feinberg MS, Scheinowitz M, Laron Z. Echocardiographic dimensions and function in adults with primary growth hormone resistance (Laron syndrome). *Am J Cardiol.* 2000;85(2):209-213.
44. Längin M, Konrad M, Reichart B, et al. Hemodynamic evaluation of anesthetized baboons and piglets by transpulmonary thermodilution: Normal values and interspecies differences with respect to xenotransplantation. *Xenotransplantation.* 2020;27(5):e12576.
45. Yakar S, Liu JL, Stannard B, et al. Normal growth and development in the absence of hepatic insulin-like growth factor I. *Proc Natl Acad Sci U S A.* 1999;96(13):7324-7329.
46. Reichart B, Längin M, Denner J, Schwinzer R, Cowan PJ, Wolf E. Pathways to clinical cardiac xenotransplantation. *Transplantation.* 2020. (accepted for publication).
47. Klymiuk N, van Buerck L, Bahr A, et al. Xenografted islet cell clusters from INSLEA29Y transgenic pigs rescue diabetes and prevent immune rejection in humanized mice. *Diabetes.* 2012;61(6):1527-1532.

## SUPPORTING INFORMATION

Additional supporting information may be found online in the Supporting Information section.

**How to cite this article:** Hinrichs A, Riedel EO, Klymiuk N, et al. Growth hormone receptor knockout to reduce the size of donor pigs for preclinical xenotransplantation studies. *Xenotransplantation.* 2020;00:e12664. <https://doi.org/10.1111/xen.12664>